

# Stereological Estimation and Zonal Distribution of the Hepatotoxic Effects of Doxorubicin on the Female Albino Rat (*Rattus Norvegicus*)

Khulud Nurani,<sup>1</sup> Anne Pulei,<sup>2</sup> Beda Olabu,<sup>3</sup> Jeremiah Munguti,<sup>4</sup> Talha Chaudhry,<sup>1</sup> Vincent Kipkorir.<sup>5</sup>

## Abstract

**Background:** Doxorubicin is an anti-neoplastic agent widely indicated for a variety of cancers. One of its adverse effects is hepatotoxicity which presents with hepatocyte necrosis, sinusoidal dilation, and fibrosis. However, there remains a dearth in the quantification and zonal distribution of this damage. **Methods:** Twenty-three adult female Wister albino rats were placed into baseline, control, and experimental group receiving 2.5mg/kg bodyweight Doxorubicin intra-peritoneally thrice weekly for 3-weeks. Rats were sacrificed on days 0, 7, 14 and 21 and livers harvested for processing. Masson's Trichrome was used in staining 7  $\mu$ m thick sections. Images were taken and analyzed via STEPanizer, and data entered into SPSS for analysis. **Results:** Rats treated with Doxorubicin had increased liver to body weight ratios from 5.00% at baseline to 6.15%, 6.69% and 7.56% on days 7, 14 and 21 ( $p=0.090$ ). There was a decrease in hepatocyte densities from 51.88/mm<sup>2</sup> to 48.61/mm<sup>2</sup>, 46.65/mm<sup>2</sup> and 42.24/mm<sup>2</sup> on day 7, 14 and 21 ( $p=0.779$ ). Collagen fiber deposition increased from 0.12 $\pm$ 0.06 cm<sup>3</sup> to 0.47 $\pm$ 0.55 cm<sup>3</sup>, 1.64 $\pm$ 0.11 cm<sup>3</sup> and 1.88 $\pm$ 0.24 cm<sup>3</sup> on days 7, 14 and 21 ( $p=0.009$ ). Deposition was greatest periportal and least pericentrally. Volume of sinusoidal spaces increased from 5.46 $\pm$ 0.50 cm<sup>3</sup> to 5.49 $\pm$ 0.15 cm<sup>3</sup>, 5.53 $\pm$ 0.24 cm<sup>3</sup> and 5.50 $\pm$ 0.17 cm<sup>3</sup> on days 7, 14 and 21 respectively ( $p=0.827$ ). Sinusoids were larger pericentrally than periportal. **Conclusion:** Doxorubicin administration is associated with an increase in volume density of fibrotic tissue and sinusoidal spaces but decrease in hepatocytes. The quantitative changes presented may facilitate histopathological grading of Doxorubicin-induced hepatotoxicity.

## Introduction

Doxorubicin is a widely indicated anti-neoplastic agent for a variety of cancers including breast cancer, bladder cancer, thyroid cancer, Kaposi's sarcoma, lymphoma, soft tissue sarcoma, multiple myeloma, and acute lymphocytic leukemia. It is the first line agent for metastatic breast cancer as well as for metastatic and locally advanced un-resectable soft-tissue sarcoma.<sup>1</sup> It is administered intravenously in dosage regimens specific to the cancer type and progression.<sup>2</sup> With regards to its mechanism of action, Doxorubicin generates free radicals during its metabolism in the liver. These free radicals disrupt normal cellular physiology and subsequently may cause toxicity in multiple organs mainly in the heart, kidneys, and liver.<sup>3</sup> Previous studies on Doxorubicin-induced hepatotoxicity have been descriptive and remain short of stereological and zonal data.<sup>4,5</sup>

Stereology is a growingly applied quantitative method used for the estimation of 3D parameters.<sup>6</sup> Because 2D profiles do not adequately depict object sizes and quantities, they are prone to inaccuracies when used in morphometric research.<sup>7</sup> As a result,

significant mistakes might be made when interpreting quantitative data from 2D profiles. Stereology provides a solution to this by providing strong mathematical methods to eliminate bias and thus accurately make 3D estimations provided sampling, randomization, and isotropy are streamlined.<sup>8</sup> Additionally, quantitative data that can show tiny variations in the volume or number of chosen parameters can be obtained using stereological procedures.<sup>7</sup> This is of high significance in analysis of liver biopsies which continue to be the gold standard for classifying liver damage.<sup>9</sup> Consequently, efforts have been made over the past few years to precisely quantify necrotic, fibrotic,<sup>10</sup> steatotic<sup>11</sup> and cancerous tissue,<sup>12</sup> both in clinical and experimental studies.<sup>13</sup> This study, therefore, sought to estimate and zonally determine the distribution of the toxic effects of Doxorubicin on the hepatic stroma and parenchyma of the female Albino rat over a 3-week period of Doxorubicin administration.

## Methods

The study was of quasi-experimental design where female albino rats were used. These were obtained from the Department of

<sup>1</sup> BSc Anat. Fourth-year Medical Student. University of Nairobi, Nairobi, Kenya.

<sup>2</sup> BSc Anat, MBChB, MSc. Anat, MMed. (Obs Gyn), MPH, University of Nairobi/Kenyatta National Hospital, Nairobi, Kenya.

<sup>3</sup> BSc Anat, MBChB, MSc. Anat, MMed (Radiology), University of Nairobi/Kenyatta National Hospital, Nairobi, Kenya.

<sup>4</sup> BSc Anat, MBChB, MSc. Anat, University of Nairobi/Kenyatta National Hospital, Nairobi, Kenya.

<sup>5</sup> BSc Anat. Fifth-year Medical Student. University of Nairobi, Nairobi, Kenya.

**About the Author:** Khulud Nurani is currently a fourth year medical student at The University of Nairobi, Nairobi, Kenya, of a six-year program. She is also a recipient of an Intercalated Degree in Human Anatomy.

### Correspondence:

Khulud Nurani.

Address: University Wy, Nairobi, Kenya

Email: [khuludnurani@gmail.com](mailto:khuludnurani@gmail.com)

Editor: Francisco J. Bonilla-Escobar  
Student Editors: Amaan Javed, Manas Pustake & Patricia Garcia-Espinosa  
Copyeditor: Sebastian Diebel  
Proofreader: Amy Phelan  
Layout Editor: Ana Maria Morales

Submission: Oct 22, 2022  
Revisions: Dec 9, 2022, Apr 4, 2023  
Responses: Jun 4 Jul 20, 2023  
Acceptance: Aug 6, 2023  
Publication: Sep 19, 2023  
Process: Peer-reviewed

Zoology and were kept and studied at the Department of Zoology Animal House. The harvested specimens were processed at the Department of Human Anatomy. These rodents were the preferred animal models for research due to their genetic, physiological, and anatomical similarity to humans, ease of maintenance, short life cycle and their small size.<sup>14</sup>

Sample size calculation was done using the formula by Charan & Biswas, 2013<sup>15</sup> using a statistical significance of 0.05, a power of 80%, a smallest meaningful difference of 1.4% and the standard deviation of 0.87% for mean liver fibrosis derived from a study by Yi et al, 2012.<sup>16</sup> A total of 23 rats were used of which two were baseline, six were controls and fifteen experimental.

Ethical approval for the study was sought from the Faculty of Veterinary Medicine (*Reference Number: FVM BAUEC/2021/286*). The study was conducted, and the animals were handled according to the guidelines provided by the committee.

Adult female albino rats of three months of age were used in the study upon selection by convenience sampling technique. Doxorubicin's commonest indication is for breast cancer, and breast cancer is more common in females than males, thus female rats were used to account for the protective effects of estrogen on the liver.<sup>17</sup> Rats with any visible pathology or abdominal injuries were excluded. The sampling technique involved randomly assigning all the rats a number between 1 and 23 using non-repeating numbers generated by Intel® Digital Random Number Generator Software. The rats were labelled using picric acid on their fur and random selection applied to split them into 3 groups, where group A was the baseline group, Group B was the control group that was administered normal saline intra-peritoneally while group C was the experimental group that was administered Doxorubicin intra-peritoneally (IP). The rats were housed in standard cages floored with wooden shavings which were replaced every two days. The cages were placed in a room with a normal 12-hour light/dark diurnal cycle. The rats were kept in their cages for 3 days for acclimatization after which intervention was begun. They were provided with standard rat pellets and water ad libitum during the study period. No additional intervention was given to reduce chemotherapy-induced distress.

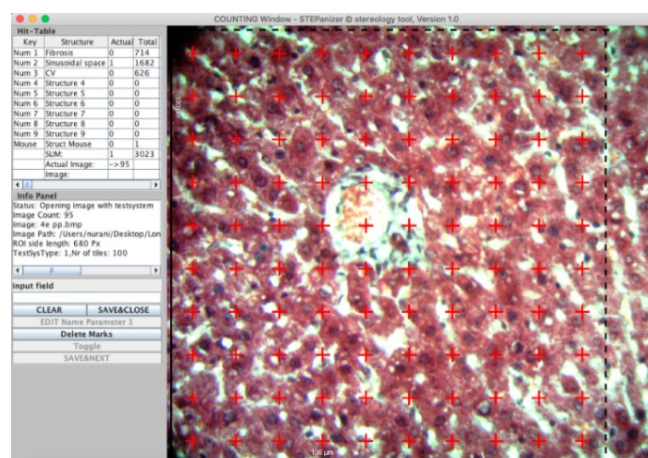
Each rat in the experimental group received 2.5 mg/kg body weight of Doxorubicin intra-peritoneally thrice weekly for three weeks (at an interval of 48 hours) to correspond with the intravenous route and timeline of administration of Doxorubicin in humans without posing toxicity to the rats. Animals in the control group received zero point five milliliters of normal saline intra-peritoneally thrice weekly as a sham. IP injections were done using a 31-gauge needle to prevent iatrogenic injury.

Tissue harvesting was done after weighing the rats using an electric measuring scale and euthanizing them by placing them in sealed containers with 1% halothane (1-3%) soaked in cotton

wool. Death was confirmed by the absence ocular reflexes. Then a longitudinal incision in the midline of the body was made and normal saline used to flush out all the blood. Thereafter, 10% formal saline was infused by the trans-cardiac method to start tissue fixation. The liver was harvested from each rat, absolute volumes calculated using Scherle's method and stored in formal saline. Systematic uniform random sampling method was used to get the liver segments. The liver was sliced across the lobes into 16 equal parts. The parts were rearranged into a diamond shape with smaller pieces arranged on either side of the largest piece of liver.<sup>9</sup> Following this, the 2<sup>nd</sup> piece was selected and thereafter every 3<sup>rd</sup> piece. A total of 5 pieces per liver were picked for histological processing.

The liver pieces obtained were placed in specimen bottles containing 10% formalin for at least 24 hours to preserve the tissues. Following fixation, they were dehydrated in ascending concentrations of alcohol, then cleared in toluene then infiltrated with paraffin wax. The embedded tissues were blocked for sectioning. They were cut into 7 µm thick sections. Every fourth section of the ribbon was selected and floated in a warm water bath to enhance spreading. The sections were fished from the water bath onto a gelatinized glass slide. They were dried at 38°C for 24 hours, then de-waxed, re-hydrated and stained using Masson's Trichrome.

**Figure 1.** STEPanizer Grid for Estimation of Volume Densities.



Out of the 10 stained sections, 5 even sections were chosen for histomorphometric analysis. Photomicrographs were taken at x400 magnification using a Richter Optica™ digital photomicroscope (Model UX1) connected to Motic Images Plus 3.0 for stereological analysis. Three images were taken per slide—one of the periportal region, one of the midzonal region and one of the pericentral region. The photomicrographs were analyzed using STEPanizer Stereology Tool Version 1.0. The estimation of volume densities and hepatocyte densities was done using Cavalieri's principle of point counting.<sup>8</sup> The histological regions were analyzed using a superimposed 100-point grid over the photomicrographs (*Figure 1*). The volume densities of the histological components were calculated and averaged to reduce

bias. Absolute volumes were then calculated by multiplying the volume densities with the liver volumes.

Data obtained were keyed into the Statistical Package for Social Sciences software (version 28.0) for statistical analysis. Hepatocytes were expressed in numbers/mm<sup>2</sup> and fibrotic tissue and sinusoidal spaces were expressed as absolute volumes. The data were grouped into three groups: A, B and C. The Shapiro-Wilk test and a visual examination of the histograms and box plots produced from the data were used to determine whether the data were normal. Although the Shapiro Wilk test indicated a normal distribution, the histograms displayed skewed distributions. Thus, non-parametric tests were employed. Kruskal Wallis test was employed to check for statistically significant differences over time in both the control and experimental groups over the study period. A Dunn Bonferroni post-hoc test was carried out. Mann Whitney U tests were carried out to assess for significant differences between the control and experimental group on each of the perfusion days. A p value of 0.05 or lower was regarded as significant. Photomicrographs were used to demonstrate the histological findings.

## Results

### General health of Study Animals

Following Doxorubicin administration, the study animals developed diarrhea, roughness in their fur coat, mucosal inflammation and tremors. They exhibited hypoactivity and reduced food intake. No discernible gross changes in livers of the experimental rats were noted when compared to the control and the baseline groups.

### Liver to Body Weight Ratio (LBWR)

The liver to body weight ratios of the control animals increased slightly over time ( $p=0.180$ ) with those of the experimental animals increasing more rapidly ( $p=0.090$ ). The difference in LBWR between controls and experimental groups was statistically significant ( $p=0.029$ ).

### Collagen fiber density

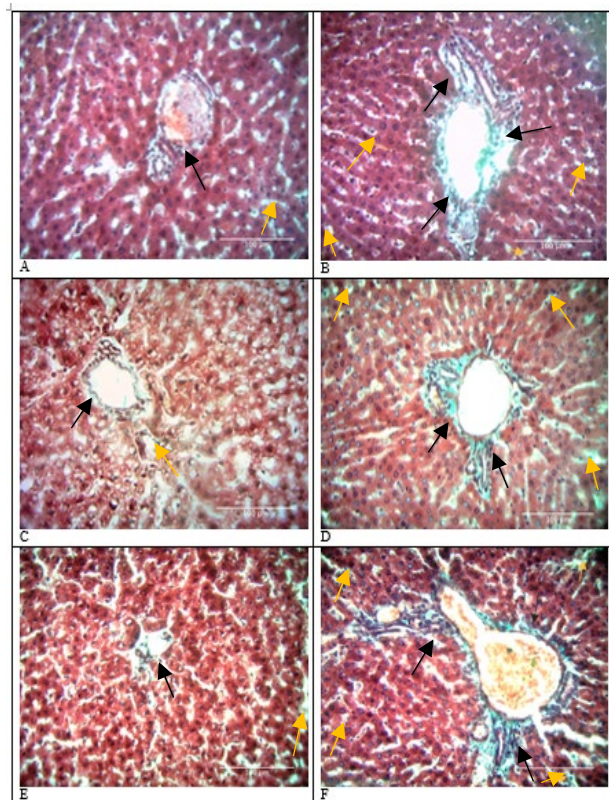
Doxorubicin administration resulted in deposition of collagen fibers in the periportal areas as well as within perisinusoidal spaces that increased with time ( $p=0.009$ ). This is illustrated in [Figures 2](#) and [3](#) below. Bridging fibrosis also developed and was most defined on day 21. In contrast, the stroma of the control group hardly had any differences in collagen fiber volumes from baseline tissues. The experiment and control groups thus, had statistically significant differences in collagen fiber volumes ( $p<0.001$ ). [Table 1](#) displays the means, standard deviations, medians, interquartile ranges and p values of the control and experimental groups over time.

### Sinusoidal space density

Doxorubicin administration resulted in an increase in volumes of sinusoidal spaces over time ( $p=0.827$ ). This is illustrated in [Figure 4](#) below. Sinusoids in the pericentral area were larger than those

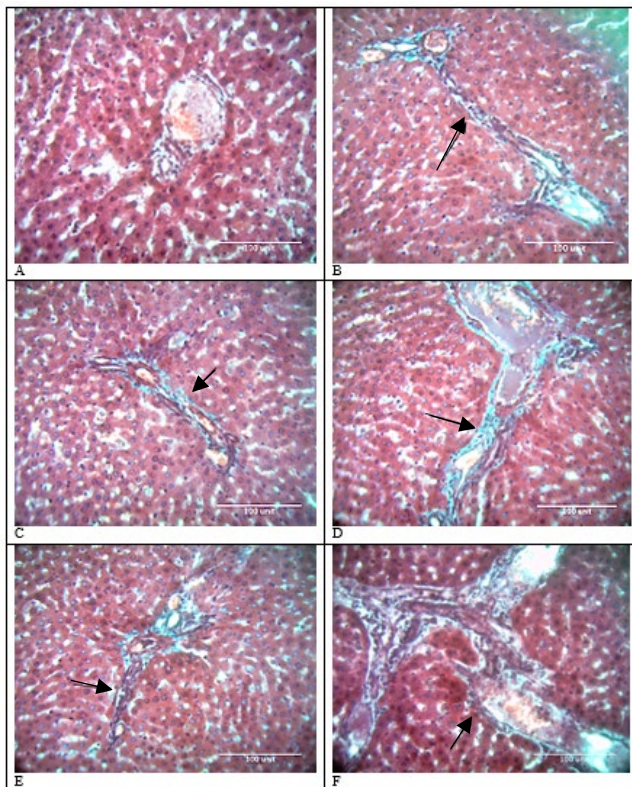
in periportal areas. In contrast, sinusoids in control tissue did not have distinct differences in sinusoidal densities from baseline tissue ( $p=1.000$ ). The experimental and controls groups did not have statistically significant differences in sinusoidal volumes ( $p=0.667$ ). [Table 2](#) displays the means, standard deviations, medians, interquartile ranges and p values of the control and experimental groups over time.

**Figure 2.** Collagen Fiber Profile in Rat Livers.



**Legend:** Figure 2A-F: Collagen Fiber Profile in the Rat Livers. Stain: Masson's Trichrome, Magnification: X 400. Figure 2A: Photomicrograph of the liver of a control rat on day 7 of the study. There are a few collagen fibers (yellow arrows) interspersed between the hepatocytes in the perisinusoidal spaces. The black arrows point at collagen fibers around the portal triad. Figure 2B: Photomicrograph of the liver of a rat treated with Doxorubicin on day 7 of the study. There are a few collagen fibers (yellow arrows) interspersed between the hepatocytes in the perisinusoidal spaces. The black arrows point at collagen fibers around the portal triad. Figure 2C: Photomicrograph of the liver of a control rat on day 14 of the study. There are a few collagen fibers (yellow arrows) interspersed between the hepatocytes in the perisinusoidal spaces. The black arrows point at collagen fibers around the portal triad. Figure 2D: Photomicrograph of the liver of a rat treated with Doxorubicin on day 14 of the study. There are collagen fibers (yellow arrows) interspersed between the hepatocytes in the perisinusoidal spaces. The black arrows point at collagen fibers around the portal triad. Figure 2E: Photomicrograph of the liver of a control rat on day 21 of the study. There are a few collagen fibers (yellow arrows) interspersed between the hepatocytes in the perisinusoidal spaces. The black arrows point at collagen fibers around the portal triad. Figure 2F: Photomicrograph of the liver of a rat treated with Doxorubicin on day 21 of the study. There are more collagen fibers (yellow arrows) interspersed between the hepatocytes in the perisinusoidal spaces. The black arrows point at collagen fibers around the portal triad.

**Figure 3.** Comparison of Bridging Fibrosis in Control and Experimental Rat Livers.



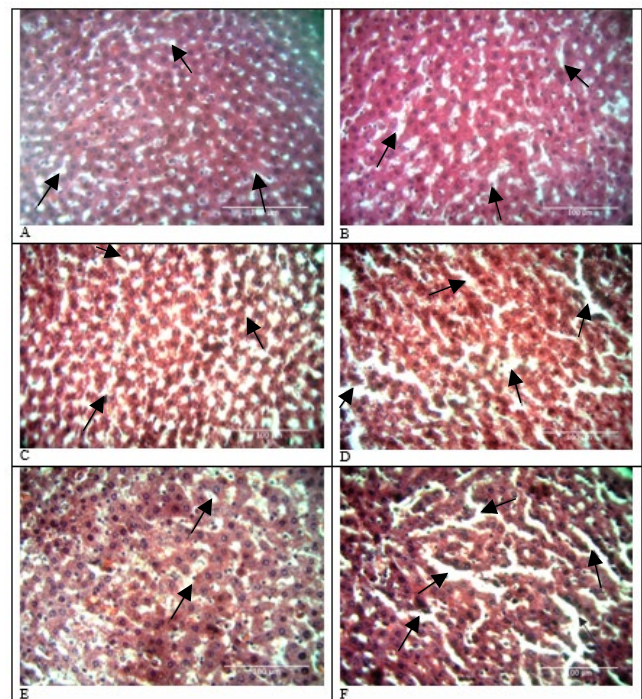
**Legend:** Figure 3A-F: Bridging Fibrosis in the Rat Livers. Stain: Masson's Trichrome, Magnification: X 400. Figure 3A: Photomicrograph of the liver of a control rat treated on day 7 of the study. There was no bridging fibrosis. Only some collagen fibers were present around the portal triad. Figure 3B: Photomicrograph of the liver of a rat treated with Doxorubicin on day 7 of the study demonstrating setting in of bridging fibrosis (black arrows). Figure 3C: Photomicrograph of the liver of a control rat on day 14 of the study demonstrating some bridging fibrosis (black arrows). Figure 3D: Photomicrograph of the liver of a rat treated with Doxorubicin on day 14 of the study demonstrating some bridging fibrosis (black arrows). Figure 3E: Photomicrograph of the liver of a control rat on day 21 of the study demonstrating some bridging fibrosis (black arrows). Figure 3F: Photomicrograph of the liver of a rat treated with Doxorubicin on day 21 of the study demonstrating the most extensive bridging fibrosis (black arrows).

**Table 1.** Volume of Fibrotic Tissue at Different Time Periods.

| Day | Group        | Volume of Fibrosis (cm <sup>3</sup> ) |                  |
|-----|--------------|---------------------------------------|------------------|
|     |              | Mean ± SD                             | Median (IQR)     |
| 0   | Baseline     | 0.12 ± 0.08                           | 0.12             |
| 7   | Control      | 0.14 ± 0.03                           | 0.14             |
|     | Experimental | 0.47 ± 0.12                           | 0.45 (0.36-0.59) |
| 14  | Control      | 0.13 ± 0.06                           | 0.13             |
|     | Experimental | 1.64 ± 0.24                           | 1.54 (1.50-1.83) |
| 21  | Control      | 0.17 ± 0.11                           | 0.17             |
|     | Experimental | 1.88 ± 0.55                           | 1.97 (1.37-2.35) |

**Legend:** Sd, Standard deviation. IQR, Interquartile range.

**Figure 4.** Comparison of Sinusoidal Spaces in Control and Experimental Rat Livers.



**Legend:** Figure 4A-F: Sinusoidal Spaces in the Rat Livers. Stain: Masson's Trichrome, Magnification: X 400. Figure 4A: Photomicrograph of the liver of a control rat on day 7 of the study. The relatively small sinusoidal spaces are illustrated with black arrows. Figure 4B: Photomicrograph of the liver of a rat treated with Doxorubicin on day 7 of the study. There are relatively larger sinusoidal spaces (Black arrows). Figure 4C: Photomicrograph of the liver of a control rat on day 14 of the study. Sinusoidal spaces, pointed at by black arrows, are smaller than those in Figure 9D. Figure 4D: Photomicrograph of the liver of a rat treated with Doxorubicin on day 14 of the study. There are larger and more distorted sinusoidal spaces (Black arrows). Figure 4E: Photomicrograph of the liver of a control rat on day 21 of the study. Sinusoidal spaces, pointed at by black arrows, are smaller than those in Figure 9F. Figure 4F: Photomicrograph of the liver of a rat treated with Doxorubicin on day 21 of the study. Sinusoidal spaces, pointed at by black arrows, are the largest and most distorted.

**Effects of Doxorubicin on the Hepatic Parenchyma**

The control rats displayed normal liver histoarchitecture. However, the experimental rats had distortions in their parenchyma. There was marked degeneration with disruption of the cord-like arrangement of hepatocytes. There was also infiltration of deeply basophilic leukocytes in the periportal area and regions of focal necrosis in the pericentral area. The hepatocytes nearer the central veins were more vacuolated than those in the periportal areas.

Hepatocyte densities declined progressively with minimum numbers recorded in the 3rd week (p=0.779). This is illustrated in [Figure 5](#) below. The periportal areas had a higher concentration of hepatocytes relative to the pericentral areas. On the other hand, hepatocyte densities for the control rats remained similar in number to those in baseline tissue (p=0.867). The differences between control and experimental values were, however, not statistically significant (p=0.178). [Table 3](#) displays the means,

standard deviations, medians, interquartile ranges and p values of the control and experimental groups over time (Table 3).

Table 2. Volume of Sinusoidal Spaces at Different Time Periods.

| Day | Group        | Sinusoidal Spaces (cm <sup>3</sup> ) |                  | p-value (vs control) Exact Sig. [2*(1-tailed Sig.)] |
|-----|--------------|--------------------------------------|------------------|---|
|     |              | Mean ± SD                            | Median (IQR)     |   |
| 0   | Baseline     | 5.46 ± 0.70                          | 5.46             | -   |
|     | Control      | 5.14 ± 0.56                          | 5.44             |   |
| 7   | Experimental | 5.49 ± 0.34                          | 5.52 (5.15-5.80) | 1.000   |
|     | Control      | 5.15 ± 0.21                          | 5.45             |   |
| 14  | Experimental | 5.50 ± 0.54                          | 5.67 (5.04-5.95) | 0.857   |
|     | Control      | 5.14 ± 0.45                          | 5.44             |   |
| 21  | Experimental | 5.50 ± 0.39                          | 5.40 (5.18-5.88) | 0.857   |

Legend: SD, Standard deviation. IQR, Interquartile range.

Figure 5. Change in hepatocyte densities over time.

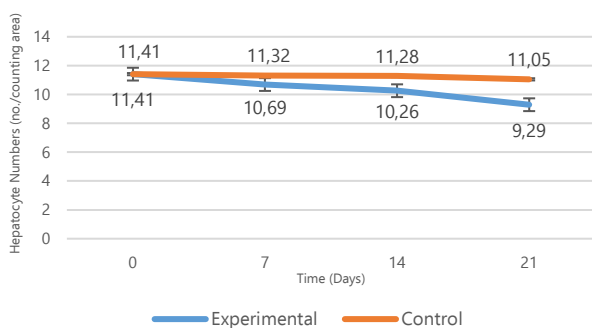


Table 3. Hepatocyte Area Densities at Different Time Periods.

| Day | Group        | Hepatocyte area densities (no./counting area) |                    | p-value (vs control) Exact Sig. [2*(1-tailed Sig.)] |
|-----|--------------|---|--------------------|---|
|     |              | Mean ± SD                                     | Median (IQR)       |   |
| 0   | Baseline     | 11.41 ± 2.24                                  | 11.41              | -   |
|     | Control      | 11.32 ± 1.09                                  | 11.32              |   |
| 7   | Experimental | 10.69 ± 1.03                                  | 10.56 (9.74-11.71) | 0.571   |
|     | Control      | 11.28 ± 0.16                                  | 11.27              |   |
| 14  | Experimental | 10.26 ± 0.65                                  | 10.13 (9.71-10.88) | 0.381   |
|     | Control      | 11.05 ± 0.72                                  | 11.05              |   |
| 21  | Experimental | 9.29 ± 4.43                                   | 6.52 (5.85-14.12)  | 0.857   |

## Discussion

The findings in this study are suggestive of a temporal increase in the deposition of collagen fibers and in sinusoidal dilatation but decrease in hepatocyte densities as discussed below. These structural changes may be helpful in grading of toxicity via liver biopsies, provide clarity on the zonal distribution of structural changes, and pave way for studies to determine strategies to reduce the severity of Doxorubicin induced hepatotoxicity.

## General health of Study Animals

The experimental rats in this study developed diarrhea, roughness in their fur coat, mucosal inflammation and tremors. These effects may be due to an inhibition of multiplication of otherwise rapidly proliferating cells of the gastrointestinal tract, skin and bone marrow by Doxorubicin.<sup>18</sup>

## Liver to Body Weight Ratio

Doxorubicin treatment resulted in an increase in the LBWR compared to that of the control rats. The increase in liver weight observed in this study following Doxorubicin is similar to the findings by Salouege et al., (2014) which found an increase in organ to body weight ratios of the heart, liver, spleen and kidneys following Doxorubicin administration in rats. The increase in liver weights corresponds to augmentative hepatomegaly which is a compensatory regenerative process following hepatocyte necrosis.<sup>20</sup> The initial phase of hepatomegaly is hypertrophy of the existing hepatocytes then later hyperplasia if regeneration is still incomplete. In this study, hypertrophy of hepatocytes could explain the increase in LBWR since a reduction in hepatocyte densities precluding regenerative hyperplasia of hepatocytes was observed. Hepatomegaly is a common adverse effect of chemotherapy and may culminate in severe liver injury and even liver failure if not controlled.<sup>21</sup>

## Collagen Fiber Density

Doxorubicin administration resulted in an increase in collagen fiber deposition in the perisinusoidal and periportal areas over time. Perisinusoidal fibrosis is postulated as being a result of hepatocyte stellate cell (HSC) activation by the reactive oxygen species (ROS) released during Doxorubicin metabolism. The activated HSC transform into highly proliferative myofibroblast-like cells with a greatly enhanced capacity to synthesize ECM components including type I and III fibrillary collagen, laminins and fibronectin.<sup>22</sup> The periportal and bridging fibrosis may be due to the activation of portal fibroblasts to form portal myofibroblasts which are pronounced for their matrix deposition and contractility.<sup>23</sup> Placement of groups of contractile cells in collagen type I matrices leads to compaction and alignment of the collagen between them, creating the appearance of bridging fibrosis. This may explain the realignment of connective tissue fibers seen in bridging fibrosis. Advancing of liver fibrosis may result in nodular regeneration, cirrhosis, and portal hypertension and often requires liver transplantation.<sup>22</sup>

## Sinusoidal Space Dilatation

Doxorubicin administration resulted in an increase in the sinusoidal space density. Injury to sinusoidal endothelial cells by ROS leads to embolization of endothelial cells and blood cells in sinusoidal spaces. This blocks venous outflow, resulting in hepatic congestion and subsequent sinusoidal dilatation. This is followed by sinusoidal obstruction syndrome characterized by fiber deposition in the sinusoids by activated HSC and obliteration of central venules.<sup>24</sup> The result is the loss of fenestrations and development of basement membranes by sinusoidal endothelial

cells in a process of capillarization, forming channels with larger calibers.<sup>25</sup> Sinusoidal obstruction syndrome can progress into regenerative nodular hyperplasia or may normalize with time after cessation of chemotherapy.<sup>21</sup> Sinusoidal obstruction causes congestion, hepatomegaly, fluid retention, jaundice and ascites, and becomes fatal in 20-50% of patients on high dose chemotherapy.<sup>26</sup>

### Effects of Doxorubicin on the Hepatic Parenchyma

Periportal leukocyte infiltration following Doxorubicin administration as observed in this study may be due to an increase in recruitment of immune cells via chemotaxis following hepatocyte injury and death.<sup>27</sup> Hepatocyte vacuolation following Doxorubicin administration, as observed in this study, was associated with larger nuclei, and is postulated as being a marker of senescence. It is present in a variety of acute and chronic liver diseases. However, the exact pathophysiology behind the vacuolation is unclear and is suggested as being the result of hydropic change.<sup>28</sup> Focal necrosis, in association with lymphocytes, as observed in this study, describes a continuum of lobular injury.<sup>29</sup>

Decrease in hepatocytes following doxorubicin administration, as observed in this study, may be a result of hepatocyte necrosis and apoptosis. The FR released during Doxorubicin metabolism reacts with hepatocyte lipids, proteins and nuclei acids causing mitochondrial dysfunction and lipid peroxidation which induces apoptosis. Following cell death, regeneration of hepatocytes is also impaired as Doxorubicin inhibits topoisomerase II activity and thus inhibiting cell division.<sup>30</sup> The result is a decline in hepatocyte numbers and distortion in the radial organization of cords. Severe hepatocyte apoptosis and necrosis may culminate into liver failure.

### Limitations and Delimitations

This study may have had some possible confounders such as inter-animal differences in the absorption and metabolism of Doxorubicin. This was, however, minimized by the use of in-bred rats which are genetically similar. Also, stress due to intraperitoneal injections may have affected the hepatic histoarchitecture. This was standardized by the administration of normal saline intraperitoneal injections in the control group. In addition, tissue shrinkage during tissue processing may have altered the normal parameters. However, errors due to tissue processing were carried through all measurements.

## References

1. Paridaens R, Biganzoli L, Bruning P, Klijn JGM, Gamucci T, Houston S, et al. Paclitaxel Versus Doxorubicin as First-Line Single-Agent Chemotherapy for Metastatic Breast Cancer: A European Organization for Research and Treatment of Cancer Randomized Study With Cross-Over. *J Clin Oncol.* 2000;18(4):724.

### Strengths of the Study

1. The histoarchitecture of the Albino rat liver very closely resembles that of humans.
2. Intermittent dosage forms administered make it analogous to Doxorubicin therapy in humans.
3. Sacrifice at the end of each week enabled establishment of temporal effects.

### Conclusion

Doxorubicin administration is associated with an increase in the volume densities of fibrotic tissue and sinusoidal spaces and decrease in hepatocyte densities. The quantitative structural changes further corroborate Doxorubicin-induced hepatotoxicity and may facilitate histopathological diagnosis of hepatotoxicity.

## Summary – Accelerating Translation

**Title:** Stereological Estimation and Zonal Distribution of the Hepatotoxic Effects of Doxorubicin on the Female Albino Rat (*Rattus Norvegicus*)

**Main Problem:** Doxorubicin is a chemotherapeutic agent widely indicated for a variety of cancers. One of its side effects is liver toxicity which presents with cellular death, vascular dilation, and fibrosis. However, there has remained a dearth in the quantification and zonal distribution of this liver damage.

**Aim:** To quantify and zonally determine the distribution of the hepatotoxic effects of Doxorubicin on the female Albino rat.

**Methodology:** Twenty-three adult female Wistar albino rats were placed into 3 groups: baseline, control and experimental. The experimental group received 2.5mg/kg bodyweight of Doxorubicin intra-peritoneally thrice weekly for 3 weeks. The control group received 0.5 ml normal saline intra-peritoneally thrice weekly as a sham. Rats were then sacrificed on days 0, 7, 14 and 21 and their livers harvested for processing and analysis.

**Results:** Rats treated with Doxorubicin had increased liver to body weight ratios from 5.00% at baseline to 6.15%, 6.69% and 7.56% on days 7, 14 and 21 ( $p=0.090$ ). There was a decrease in hepatocyte densities from 51.88/mm<sup>2</sup> to 48.61/mm<sup>2</sup>, 46.65/mm<sup>2</sup> and 42.24/mm<sup>2</sup> on day 7, 14 and 21 ( $p=0.779$ ). Collagen fiber deposition increased from 0.12±0.06 cm<sup>3</sup> to 0.47±0.55 cm<sup>3</sup>, 1.64±0.11 cm<sup>3</sup> and 1.88±0.24 cm<sup>3</sup> on days 7, 14 and 21 ( $p=0.009$ ). Deposition was greatest periportal and least pericentrally. Volume of sinusoidal spaces increased from 5.46±0.50 cm<sup>3</sup> to 5.49±0.15 cm<sup>3</sup>, 5.53±0.24 cm<sup>3</sup> and 5.50±0.17 cm<sup>3</sup> on days 7, 14 and 21 respectively ( $p=0.827$ ). Sinusoids were larger pericentrally than periportal.

**Conclusion:** Doxorubicin administration is associated with an increase in volume density of fibrotic tissue and sinusoidal spaces but decrease in hepatocyte densities. The quantitative changes presented may facilitate histopathological grading of doxorubicin-induced hepatotoxicity.

2. Johnson-Arbor K, Dubey R. Doxorubicin. In: StatPearls. Treasure Island (FL): StatPearls Publishing. Available from: <http://www.ncbi.nlm.nih.gov/books/NBK459232/>. Cited 2021 Jun 15.
3. Thorn CF, Oshiro C, Marsh S, Hernandez-Boussard T, McLeod H, Klein TE, et al. Doxorubicin pathways: pharmacodynamics and adverse effects. *Pharmacogenet Genomics.* 2011;21(7):440–6.

4. Al-Qzazz MM, Al-Sammak MA, Taher MT. Effect of Doxorubicin on the Histological Structure of the Liver in Male Albino Rats = تأثير عقار الدوكسوروبيسين على التركيب النسيجي لكبد الجرذان. *Jordan Med J.* 2013;47(3):220–6.
5. Al-Saleem IA, Jumaa HJ, Al-Ani IM, Ismael HK. Morphological Changes in the Liver of Rats (*Rattus norvegicus*) treated with different Doses of Doxorubicin. 2017;16:9.
6. Kipanyula MJ, Sife AS. Global Trends in Application of Stereology as a Quantitative Tool in Biomedical Research. *BioMed Res Int.* 2018;2018:1–9.
7. Marcos R, Monteiro RAF, Rocha E. The use of design-based stereology to evaluate volumes and numbers in the liver: a review with practical guidelines: Design-based stereology in hepatology. *J Anat.* 2012;220(4):303–17.
8. Mandarim-de-Lacerda CA. Stereological tools in biomedical research. *An Acad Bras Ciênc.* 2003;75(4):469–86.
9. Marcos R, Bragança B, Fontes-Sousa AP. Image Analysis or Stereology: Which to Choose for Quantifying Fibrosis? *J Histochem Cytochem.* 2015;63(9):734–6.
10. Vertemati M, Minola E, Goffredi M, Sabatella G, Gambacorta M, Vizzotto L. Computerized morphometry of the cirrhotic liver: Comparative analysis in primary biliary cirrhosis, alcoholic cirrhosis, and posthepatic cirrhosis. *Microsc Res Tech.* 2004;65(3):113–21.
11. Catta-Preta M, Mendonca LS, Fraulob-Aquino J, Aguila MB, Mandarim-de-Lacerda CA. A critical analysis of three quantitative methods of assessment of hepatic steatosis in liver biopsies. *Virchows Arch.* 2011;459(5):477–85.
12. Vertemati M, Vizzotto L, Moscheni C, Dhillon A, Dhillon A, Quaglia A. A morphometric model to minimize subjectivity in the histological assessment of hepatocellular carcinoma and its precursors in cirrhosis. *Microsc Res Tech.* 2008;71(8):606–13.
13. Dahab GM, Kheriza MM, El-Beltagi HM, Fouda AMM, El-Din OAS. Digital quantification of fibrosis in liver biopsy sections: Description of a new method by Photoshop software. *J Gastroenterol Hepatol.* 2004;19(1):78–85.
14. Vdoviaková K, Vdoviaková K, Petrovová E, Krešáková L, Maloveská M, Teleky J, et al. Importance Rat Liver Morphology and Vasculature in Surgical Research. *Med Sci Monit.* 2016;22:4716–28.
15. Charan J, Biswas T. How to Calculate Sample Size for Different Study Designs in Medical Research? *Indian J Psychol Med.* 2013;35(2):121–6.
16. Yi E tong, Liu R xia, Wen Y, Yin C hong. Telmisartan attenuates hepatic fibrosis in bile duct-ligated rats. *Acta Pharmacol Sin.* 2012 Dec;33(12):1518–24.
17. Ly D, Forman D, Ferlay J, Brinton LA, Cook MB. An international comparison of male and female breast cancer incidence rates. *Int J Cancer.* 2013;132(8):1918–26.
18. Mitchison TJ. The proliferation rate paradox in antimetabolic chemotherapy. *Kellogg D. Mol Biol Cell.* 2012;23(1):1–6.
19. Salouge I, Ali R, Saïd D, Elkadri N, Kourda N, Lakhel M, et al. Means of evaluation and protection from doxorubicin-induced cardiotoxicity and hepatotoxicity in rats. *J Cancer Res Ther.* 2014;10(2):274.
20. Michalopoulos GK. Principles of liver regeneration and growth homeostasis. *Compr Physiol.* 2013;3(1):485–513.
21. Maor Y, Malnick S. Liver Injury Induced by Anticancer Chemotherapy and Radiation Therapy. *Int J Hepatol.* 2013;2013:1–8.
22. Bataller R, Brenner DA. Liver fibrosis. *J Clin Invest.* 2005;115(2):209–18.
23. Forbes SJ, Parola M. Liver fibrogenic cells. *Best Pract Res Clin Gastroenterol.* 2011;25(2):207–17.
24. Sharma A, Houshyar R, Bhosale P, Choi JI, Gulati R, Lall C. Chemotherapy induced liver abnormalities: an imaging perspective. *Clin Mol Hepatol.* 2014;20(3):317.
25. Brancatelli G, Furlan A, Calandra A, Dioguardi Burgio M. Hepatic sinusoidal dilatation. *Abdom Radiol.* 2018;43(8):2011–22.
26. Fan CQ, Crawford JM. Sinusoidal obstruction syndrome (hepatic veno-occlusive disease). *J Clin Exp Hepatol.* 2014;4(4):332–46.
27. El-Sayyad HI, Ismail MF, Shalaby FM, Abou-El-Magd R, Gaur RL, Fernando A, et al. Histopathological effects of cisplatin, doxorubicin and 5-fluorouracil (5-FU) on the liver of male albino rats. *Int J Biol Sci.* 2009;466–73.
28. Nayak NC, Sathar SA, Mughal S, Duttgupta S, Mathur M, Chopra P. The nature and significance of liver cell vacuolation following hepatocellular injury? An analysis based on observations on rats rendered tolerant to hepatotoxic damage. *Virchows Arch.* 1996;428(6).
29. Krishna M. Patterns of necrosis in liver disease: Patterns of Necrosis in Liver Disease. *Clin Liver Dis.* 2017;10(2):53–6.
30. Box VGS. The intercalation of DNA double helices with doxorubicin and nagalomycin. *J Mol Graph Model.* 2007;26(1):14–9.

### Acknowledgments

Jimmy Gakure, Felix Mburu, Noel Odero.

### Conflict of Interest Statement & Funding

The Authors have no funding, financial relationships or conflicts of interest to disclose.

### Author Contributions

Conceptualization, Methodology: KN, TC. Investigation, Writing – Original Draft: K.N. Writing – Review & Editing: VK. Funding, Resources: KN. Supervision: AP, BO, JM.

### Cite as

Nurani K, Pulei A, Olabu B, Munguti J, Chaudhry T, Kipkorir V. Stereological Estimation and Zonal Distribution of the Hepatotoxic Effects of Doxorubicin on the Female Albino Rat (*Rattus Norvegicus*). *Int J Med Stud.* 2023 Jul-Sep;11(3):184–90.

*This work is licensed under a [Creative Commons Attribution 4.0 International License](https://creativecommons.org/licenses/by/4.0/)*

ISSN 2076-6327

This journal is published by [Pitt Open Library Publishing](https://open.library.utoronto.ca/pitt/)

